tension, indicating that the cranial end of the catheter was entrapped in subcutaneous tissues. A percutaneous V-18 guide wire was then advanced through the cranial end of the catheter into the RA. A 4-mm × 10-cm Sterling balloon (Boston Scientific) was advanced over the wire and was used to break tissue adhesions with forceful traction and release. This balloon ruptured and became entrapped inside the catheter lumen during extraction. A transfemoral Needle's Eye snare (Cook, Bloomington, Indiana) captured the catheter in a more cephalad location in a more stable position. The Needle's Eye snare was tightened on the catheter fragment and wire, kinking it slightly. Firm retraction of the snare removed the entire catheter fragment along with the ruptured balloon (**Fig E1** [available online on the article's Supplemental Material page at *www.jvir.org*]).

In the first patient, both catheters were encased in calcified fibrotic tissue except for the distal 1–2 cm in the RA. Traction on the subcutaneous exposed end was therefore not transmitted to the cardiac end of the catheter, but segmental inflation and traction resulted in incremental freeing of pericatheter adhesions. In a similar way, traction on the kinked 0.018-inch wire within the port catheter in the second case concentrated traction force on the unstretchable wire, reduced traction on the catheter itself, and maintained through-catheter security in case of catheter fracture. In both patients, catheter tips deep to the clavicle were accessed percutaneously with placement of robust 0.018-inch guide wires to allow sheath placement and subsequent successful removal.

Given the near-unyielding encasement of such catheter fragments, appropriately sized noncompliant high-pressure angioplasty balloons, with aggressive traction, are required to disrupt the fibrous attachments along the catheter length. Angioplasty balloons are not designed to withstand traction in the inflated state, and the authors have had success in removing entrapped catheter fragments only with noncompliant balloons. The smaller-diameter, longer balloons used in both cases described here inevitably ruptured.

In conclusion, traditional extraction techniques may fail to remove catheters bound to thrombosed, contracted veins by dense calcified adhesions along most of their length. Entrapped fragments can be treated by applying focal traction to short segments of the catheter in a reciprocating motion, applying such traction on sequential segments of the catheter until the entire trapped segment has been treated, and then extracting the balloon catheter and fragment through a percutaneous sheath or cutdown site.

ACKNOWLEDGMENTS

The authors acknowledge Casey J. Yu for her aid in editing the manuscript and assisting with submission of the manuscript.

REFERENCES

1. Busch JD, Herrmann J, Heller F, et al. Follow-up of radiologically totally implanted central venous access ports of the upper arm: long-term complication in 127,750 catheter-days. AJR Am J Roentgenol 2012; 199:447–452.
2. Desai SS, Konanur M, Foltz G, Malaisrie SC, Resnick S. An endovascular approach to the entrapped central venous catheter after cardiac surgery. Cardiovasc Intervent Radiol 2016; 39:453–457.
3. Quaretti P, Galli F, Fiorina I, et al. A refinement of Hong's technique for the removal of stuck dialysis catheters: an easy solution to a complex problem. J Vasc Access 2014; 15:183–188.
4. Ryan S, Hadziomerovic A, Aquino J, Cunningham I, O'Kelly K, Rasuli P. Endoluminal dilation technique to remove "stuck" tunneled hemodialysis catheters. J Vasc Interv Radiol 2012; 23:1089–1093.

Re: Tumor Targeting and Three-Dimensional Voxel-Based Dosimetry to Predict Tumor Response, Toxicity, and Survival after Yttrium-90 Resin Microsphere Radioembolization in Hepatocellular Carcinoma

From: Stephan Walrand, PhD
Carlo Chiesa, PhD
Pablo Minguez Gabina, PhD
Nicolas Chouin, PhD
Jonathan Gear, PhD
Caroline Stokke, PhD
Peter Bernhardt, PhD
Katarina Sjogreen Gleisner, PhD
Lidia Strigari, PhD
Mark Konijnenberg, PhD
EANM Dosimetry Committee
Nuclear Medicine (S.W.)
Cliniques Universitaires Saint-Luc
Avenue Hippocrate 10
1200 Brussels, Belgium;
Nuclear Medicine (C.C.)
Foundation Istituto di Ricovero e Cura a Carattere Scientifico
National Tumour Institute
Milan, Italy;
Department of Medical Physics and Radiation
Protection (P.M.G.)
Gurutzeta/Cruces University Hospital
Barakaldo, Spain;
Oniris, Cancers Animaux, Modèle pour la Recherche en
Oncologie Comparée (N.C.)
L'Université Nantes Angers Le Mans
Nantes, France;
Joint Department of Physics (J.G.)
Royal Marsden Hospital and Institute of Cancer Research
Sutton, United Kingdom;
Department of Diagnostic Physics (C.S.)
Oslo University Hospital
Oslo, Norway;
Department of Radiation Physics (P.B.)

S.W.'s e-mail: stephan.walrand@uclouvain.be

https://doi.org/10.1016/j.jvir.2019.08.030

Göteborg University, Sahlgrenska University Hospital
Gothenburg, Sweden;
Department of Medical Radiation Physics (K.S.G.)
Clinical Sciences Lund, Lund University
Lund, Sweden;
Department of Medical Physics (L.S.)
St. Orsola Malpighi University Hospital
Bologna, Italy; and
Department of Radiology and Nuclear Medicine (M.K.)
Erasmus University Medical Center
Rotterdam, The Netherlands

Editor:

We read with great interest the paper of Allimant et al (1) recently published in the *Journal of Vascular and Interventional Radiology*. Beside the clinical predictions of the paper, which look valuable, we are disappointed by the feeling that, motivated by the development of simple tools, mathematics becomes more and more overlooked in clinical dosimetry, resulting in hollow formalism.

In this paper (1), the authors introduced the area under the dose–volume histogram (DVH; AUDVH) formalism. The authors claimed that "AUDVH mathematically provides a better reflection of the actual dose received by the tumor than the commonly used mean dose, which does not take into account the heterogeneity of dose deposition."

However, AUDVH is nothing but the tissue mean absorbed dose!

Indeed, AUDVH is the sum of all the bins of the DVH. Each voxel i appears in the DVH up to the bin corresponding to its absorbed dose D_i, ie, D_i fold, for a volume fraction 1/N where N is the number of voxels in the tissue. Thus, each voxel contributes Di/N to AUDVH. As a result, AUDVH is trivially the tissue mean absorbed dose. Here we present a rigorous mathematical proof and an illustrating example.

As a mathematical proof, let us assume ρ(D) to be the absorbed dose distribution inside a tissue, ie, ρ(D) dD is the volume fraction of tissue having an absorbed dose between D and D + dD. By definition, we have:

$$\int_0^\infty dD\ \rho(D) = 1 \qquad \text{(Eq. 1)}$$

And the tissue mean absorbed dose $\overline{D}$ is given by:

$$\int_0^\infty dD\ \rho(D)\ D = \overline{D} \qquad \text{(Eq. 2)}$$

The DVH(D) indicating the fractional volume with an absorbed dose D or higher is:

$$DVH(D) = \int_D^\infty dD'\ \rho(D') \qquad \text{(Eq. 3)}$$

Note that DVH(0) = 1 and $\lim_{D\to\infty} DVH(D) = 0$. By integrating **Eq. 3** over D, we get the alleged AUDVH:

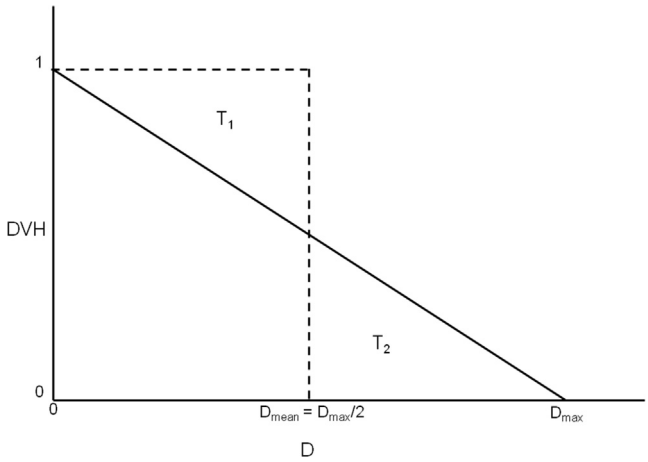

Figure. Linear decreasing DVH (solid line) and uniform DVH (dashed line) having the same mean absorbed dose ($D_{max}/2$) and same AUDVH. Furthermore, both AUDVHs are equal to this mean absorbed dose, as the triangles T_1 and T_2 have equal areas.

$$AUDVH = \int_0^\infty dD \int_D^\infty dD'\ \rho(D') \qquad \text{(Eq. 4)}$$

Inversion of the integration order according to the Fubini theorem (2) leads to:

$$AUDVH = \int_0^\infty dD'\ \rho(D') \int_0^{D'} dD \qquad \text{(Eq. 5)}$$

The integration on D is trivial and results in:

$$AUDVH = \int_0^\infty dD'\ \rho(D')\ D' = \overline{D} \qquad \text{(Eq. 6)}$$

Thus, AUDVH is nothing but the tissue mean absorbed dose.

As an example illustration for nonmathematicians, let us illustrate this general property in a basic example: the **Figure** shows 2 simple DVHs. In this case, trivial geometric considerations directly show that the AUDVH of the linear decreasing DVH (solid line) is equal to that of the uniform DVH (dashed line), both AUDVHs being equal to $D_{max}/2$, which is also the mean absorbed dose of the 2 DVHs.

In conclusion, to prevent confusion, the AUDVH terminology should be discarded and its spreading avoided in dosimetry studies.

REFERENCES

1. Allimant C, Kafrouni M, Delicque J, et al. Tumor targeting and three-dimensional voxel-based dosimetry to predict tumor response, toxicity, and survival after yttrium-90 resin microsphere radioembolization in hepatocellular carcinoma. J Vasc Interv Radiol 2018; 29:1662–1670.
2. Nykamp DQ. Examples of changing the order of integration in double integrals: example 2. Math Insight. Available at: https://mathinsight.org/double_integral_change_order_integration_examples. Accessed October 16, 2019.